

Flow characteristics around a row of circular and wavy cylinders

K. Lam*, T. Cai, Y. F. Lin and Y. Liu

*Department of Mechanical Engineering,
The Hong Kong Polytechnic University, Hung Hom, Kowloon, Hong Kong*

(Manuscript Received May 7, 2007; Revised July 2, 2007; Accepted July 11, 2007)

Abstract

The near-wake and flow interference around a row of five circular cylinders, staggered wavy cylinders and non-staggered wavy cylinders are investigated experimentally by using PIV and LIF techniques. The effects and characteristics of employing wavy cylinders instead of circular cylinders are discussed. The cylinders were arranged at $T/d=1.5$ with Re ranging from 125 to 40000. Results showed the staggered wavy cylinders give rise to a more stable flow pattern with less fluctuation and longer wake vortex closure length.

Keywords: Circular cylinders; Near-wake flow patterns

1. Introduction

Flow induced vibrations due to vortex shedding in heat exchanger tubes have stimulated extensive investigations in the past four decades. An enormous number of papers have been published to report the investigations both experimentally and numerically for a variety of tube arrangements.

The investigations on suppression of tube vibration have been carried out based on a variety of ideas. One approach focuses attention on the topic of the effective control of vortex shedding from bluff bodies. Zdravkovich [1] summarized three categories for suppressing vortex shedding from a cylinder. One of the methods is by introducing a three-dimensional geometric disturbance to the base form of a normally two-dimensional bluff body. Ahmed et al. [2] studied the effects of different wavy cylinders in a transverse flow and reported on the surface pressure distribution. They also investigated the wake and the topology of the boundary and turbulence structure behind a wavy

cylinder [3]. Lam et al. [4] investigated different wavy cylinders experimentally. They discovered that a significant reduction of drag and suppression of vibration for certain geometrical shape of the wavy cylinder. The mechanism of drag reduction and corresponding cylinder vibration was also discussed. Lam et al. [5] furthermore carried out the numerical simulation to investigate the mechanism of drag reduction and the suppression of fluctuating lift due to the wavy cylinder. The effects of altering the geometrical parameters of a single wavy cylinder subjected to cross flow were investigated. Lee et al. [6] reported that in some specified cases up to 22% of reduction of drag coefficient could be obtained for $Re=10000$ in comparison with the circular cylinder.

Based on the above findings, it is anticipated that by replacing the circular cylinders with wavy cylinders in heat exchangers, the effects of flow induced vibration of tubing could be minimized. However, when the spacing ratio between the cylinders is small, the effect of flow interference is significant. Therefore, it is necessary to study whether and how the advantages of replacing circular cylinders with wavy cylinders could be extended to a

*Corresponding author. Tel.: +852 2766 6649, Fax.: +852 2365 4703
E-mail address: mmklam@polyu.edu.hk

closely packed tube bundle with spacing ratio around $T/d=1.5$.

Besides, there has been substantial interest in the metastable flow patterns behind a single row of tubes. Corrsin [7] noticed the random fashion of the adjacent jets exit from closely spaced rods at $T/d=1.17$. Roberts [8] carried out experiments to investigate the narrow and wide flow structure around flexibly mounted tubes. Cowdrey [9] measured the base-pressure of sixteen tubes in a single row. He showed an uneven pressure coefficient diagram for $T/d=1.5$, which also showed sudden pressure change occurring intermittently. Bradshaw's [10] showed that irregular wide and narrow wakes appeared in the near wake of one row of ten tubes at $T/d=1.7$ and $Re=1.5 \times 10^3$. [11], and Akilli et al. [12] showed the same phenomenon on eight and three tubes in a row, respectively.

The current work is aimed at examining the flow interference effects of employing a row of wavy cylinders in side-by-side arrangements at small spacing ratio. Experiments were conducted to compare the near wakes of five side-by-side circular cylinders, staggered wavy cylinders and non-staggered wavy cylinders for Reynolds number ranging from 125 to 40000. PIV and LIF techniques were employed. A spacing ratio of $T/d=1.5$ was selected. The metastable issue was also studied around both the circular and wavy cylinders arrangements.

2. Experimental setup and techniques

The experiments were carried out in a closed-loop water tunnel with the test section of width $W=300\text{mm}$, height $H=600\text{mm}$ and length $L=2100\text{mm}$. The walls of the test-section were made of acrylic plates in order to provide clear view for Particle Image Velocimetry (PIV) and Laser Induced Fluorescence (LIF) experimentations. Two pumps with one electric control system were equipped to generate a desired mean flow in the test section. The free stream velocity in the testing area could be continuously adjustable from 0 to 4m/s. An overview of the experimental system with the setup of PIV equipment is shown in Fig. 1. The cylinders were assigned by numbers 1-5 from the top. The geometry of a wavy cylinder is described by the sinusoidal equation as follows:

$$d_z = d + 2a \cdot \cos(2\pi z/\lambda).$$

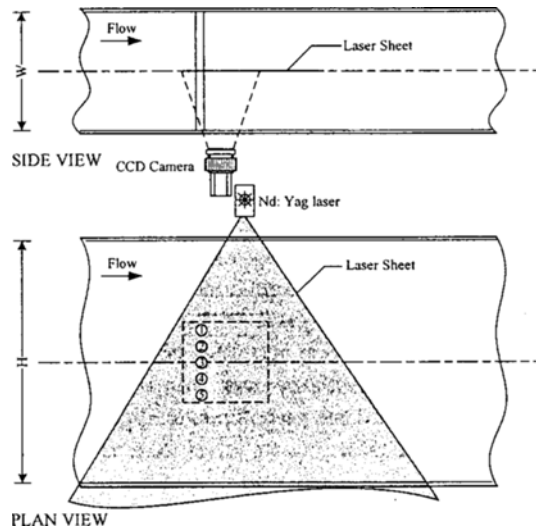


Fig. 1. Schematic diagram of the experimental setup.

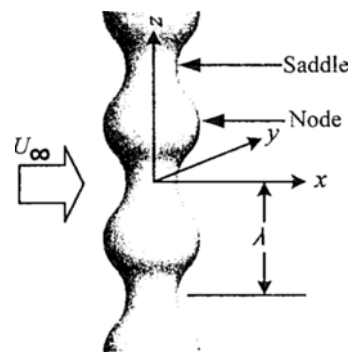


Fig. 2. Geometry of the wavy cylinder.

Referring to the numerical simulation results by Lam et al. [5], the optimal dimensionless parameters of the wavy cylinder were selected in order to produce better drag reduction at high Reynolds number. In the present investigation, the mean diameter d is 20mm, $a/d=0.15$ and $\lambda/d=1.5$. Fig. 2 shows the terminology in describing the wavy cylinder. The "saddle" denotes the minimum diameters, whereas the "node" represents the maximum diameter location. Two sets of aluminum wavy cylinders were processed with a phase shift of $\pi/2$ in order to provide perfectly staggered and non-staggered arrangements between two parallel plates. The spacing ratio of cylinders were fixed at $T/d=1.5$.

Because of the periodical variation of the cross-section of wavy cylinders, two measure planes were set for both staggered and non-staggered wavy cylinder arrangements in order to obtain adequate

information of the whole flow field. As shown in Fig. 3, the measurement planes are marked by the purple slices. Measurement plane (1) is located at the mid-span of circular cylinders. (2)-(5) corresponding to the planes, where the nodes and saddles were located of wavy cylinders.

The flow patterns of the five side-by-side circular cylinders were studied by using Laser Induced Fluorescence (LIF) visualization technique. A SONY digital video camera (DCR PC120E) was used to capture the fluid motion into video tapes. A software Microsoft Movie Maker was then employed to transform the videos from tapes to digital format (.wmv files) at 25fps.

The full field velocity vector measurements were carried out with a Dantec PIV system. One CCD camera with a resolution of 1280×1024 pixels was employed to capture the instantaneous pictures. Each picture covers an area with the dimension $239\text{mm} \times 299\text{mm}$. A Dantec control unit was used to synchronize the CCD camera with a Dantec Nd: Yag laser generator, which illuminates the measurement planes. The flow was seeded with Dante $50\ \mu\text{m}$ polyamid seeding particles. The software Dantec Flow Manager was employed for post-process purpose. Velocity vectors could then be obtained by calculating the particle movements of two consecutive pictures of the measurement planes. The parameters were set to 32×32 rectangular interrogation areas with 25% overlap in both the horizontal and vertical directions.

Based on over 150 PIV pictures of each case, a statistics process was applied to access further information. The statistics mean velocity of each point is defined as the average of the instantaneous velocity of the same point. The standard deviation of u and v , which could be employed to estimate the fluctuation of velocity in x and y directions respectively,

can subsequently be obtained and normalized by the mean flow velocity of each point. The standard deviation of v is basically proportional to that of u and will not be presented.

3. Results and discussion

Fig. 4 shows the typical flow pattern obtained from numerical simulation and flow visualization using LIF at $Re=125$ and $T/d=1.5$. As a result of flow interference at such spacing ratio, no individual Karman's vortex street can be observed behind cylinders 2-4. There is only one wide wake behind the middle cylinder (cylinder 3); the two free shear layers from cylinder 3 radiate outwards forming a wide wake behind it, while the top and bottom wakes behind cylinder 1 and 5 maintain a vortex shedding flow pattern so that the rest of the two wakes (behind cylinder 2 and 4) are squeezed by the adjacent shear layers of the gap jets to form a tadpole-like wake structure. Wakes behind cylinders 1, 2, 4 and 5 are deflecting sideward to the outer free streams. This kind of flow pattern is referred to here as a typical "stable" flow pattern for such configuration based on all the observations. Such typical flow pattern is also confirmed by the numerical simulation result on laminar flow [Fig. 4(a)].

The metastable flow patterns, which are contrary to the above stable one, are the flow patterns with a wide wake occurring behind cylinders in random manner and not only confined to the middle one.

In the case of five circular cylinders, metastable flow patterns could be observed frequently at $Re \leq 1100$. If the free stream velocity is adjusted cautiously and gradually to the target point, the wide wake will form behind the middle cylinder in all tests. Otherwise, if the free stream speed is increased or decreased rapidly, the position of wide wake will become unpredictable, i.e., the metastable flow

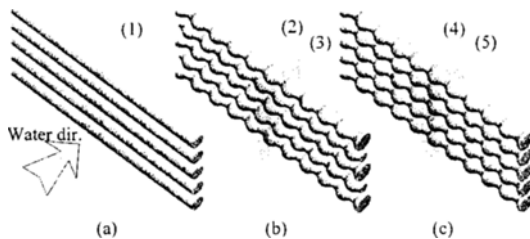


Fig. 3. Five measurement planes, (a) circular cylinders, (b) staggered wavy cylinder arrangement, (c) non-staggered wavy cylinder arrangement.

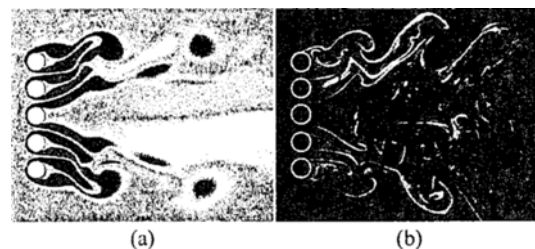


Fig. 4. Numerical simulation and flow visualization results for circular cylinders at $Re=125$ and $T/d=1.5$, (a) vorticity contour from numerical simulation, (b) LIF image.

pattern appears. When $Re > 1100$, the metastable structure could rarely be captured. Once a metastable state has been obtained under $Re \leq 1100$, it may randomly transit to the “stable” status with the free stream speed being increased to $Re > 1100$. In every case, there is only one wide wake occurring each time.

The digital video records of FIV show strong interactions among the wakes of five cylinders. Figures 4(b) and 5 present four overall instantaneous images at $Re = 125, 800$ and 3800 . Figure 6 displays two images of the upper half of the measurement plane at $Re = 125$ and $Re = 3800$.

At low Reynolds number, the whole flow pattern of the wake downstream is symmetrical about the central axis [Fig. 4 (b), Fig. 5(a)]. However, the feature of symmetry fades away gradually with the increasing of Reynolds number [Fig. 5(b), Fig. 5(c)]. The wide wake behind cylinder 3 is far from a Karman vortex street. The shedding and traveling of small vortices due to free shear layer instability are associated with the large scale reverse flow, the wakes of cylinder 2 and 4 and finally coalesce with the wakes of cylinder 1 and 5.

Marked by arrows in Fig. 5(a) and (b), the free shear layer behind cylinder 3 moves at an inclined angle, rolls up to a big vortex and forms a wide wake. Bulky reverse flows forming a horn-like structure in the middle part of wake are thus shaped. The scale of the wakes formed by the free shear layers of cylinder 2 and 3 will become shorter with increasing Reynolds number due to the increasingly biased flow degree of the jet flow between cylinders 2 and 3.

Marked by A in Fig. 5(a), the scale of the shedding vortices from cylinder 3 is quite petite. It is estimated to around half the diameter of a cylinder at most. After rolling downstream for a very short distance, A fails to amalgamate with C or C_1 , which were shedding from cylinder 1. Sometimes, it will collapse after being absorbed by the reverse flow, or be entrained outwards to form the lower part of the

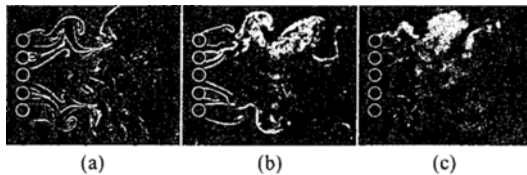


Fig. 5. Transition of flow patterns with Reynolds number, (a) $Re = 125$, (b) $Re = 800$, (c) $Re = 3800$.

vortex shedding originally from cylinder 1.

The vortices shedding from cylinders 1 and 5 are anti-phase. Taking cylinder 1 as an example, firstly, the flow forms a deflected Karman vortex street-like structure in the very near wake. The two consecutive vortices, marked as C and C_1 could be identified. As they are moving downstream, C_1 appears to be entrained by the rear part of C, the “tail” that is moving upward from the free shear layer of the cylinder 3 marked by B, and, the vortex A synchronizing with B. Finally, the lower vortex C_1 will be absorbed by the vortex C, then attach to form a lower part of it and roll up downstream.

The free shear layers around cylinder 2 and 4 could not even generate vortices at all. The wake behind cylinder 2 and 4 is strongly shaped by the jet flow from adjacent gaps. The shear layers coalesce quickly in the rear, forming a tadpole tail like vortex sheet. The swinging movement of the ‘tail’ in the very near wake ($\sim 3.5d$) is synchronous with the free shear layers nearby.

As a matter of fact, the relationship among A, B and C_1 is quite subtle. Initially, the gap vortex A leads B in the near wake. The upward movements of A and B occupy the space and disrupt the evolution of C_1 . When moving downstream, point B will be pushed to a position which is very close to the abdomen of C and then being sucked in quickly by C and rolls up with it.

Fig. 7 shows the typical mean velocity maps of the near flow field for circular cylinders, staggered and non-staggered wavy cylinders arrangements at

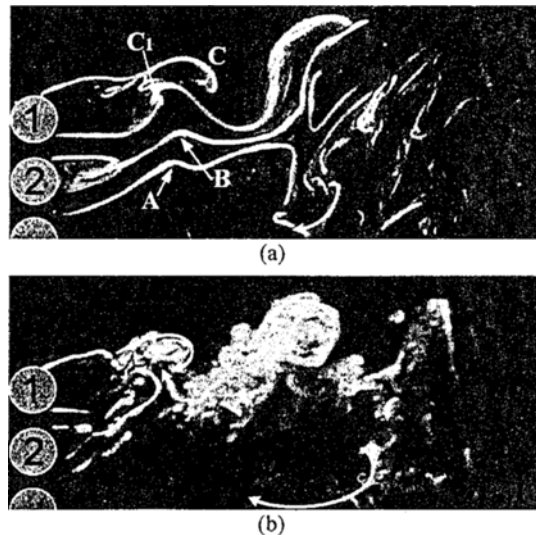


Fig. 6. Typical flow patterns, (a) $Re = 125$, (b) $Re = 3800$.

$Re=1100$. Fig. 8 shows the statistical mean streamline topology downstream of the circular and wavy cylinders at $Re=1100$, 3800 and 20000. Fig. 9 is the corresponding normalized standard deviation contours of the velocity distribution with range from 0 to 0.035 and an incremental value of 0.0025 in 15 levels. Figs. 8(a) and 9(a) are results corresponding to Fig. 6. Bracket numbers indicating the measurement planes are the ditto marks with that indicated in Fig. 3(b).

From Fig. 7, jet flows can be observed to be exiting from every gap of cylinders except at the nodal plane of non-staggered wavy cylinders arrangement. Adjacent jets coalesce immediately. In the case of non-staggered wavy cylinders arrangement, the wide wake expands and the tadpole-like structure could hardly be identified in the nodal plane [plane (4)]. It is obvious that the reverse flow is much more severe than in the other planes and responsible for the expansion of the wide wake. The reverse flow occupies a vast channel area and strikes the cylinders from rear side in a high speed that even block off the jet flows. The wide wake holds its position in the middle all the time. On the contrary, the uncertainty of the location of the wide wake in the saddle plane [plane (5)] is even more remarkable than the circular cylinder arrangement.

The mean streamline topologies show the irregular convolution of plane (4) and (5). The corresponding normalized standard deviation contour of the node plane reveals that the deviation value of each instantaneous velocity vector in the near wake far exceeds that of the other planes, which indicates a fierce disturbance of flow field in this plane. Whereas, the flow field in the downstream of the saddle plane is relatively placid. This may be due to the size of gaps between cylinders in this plane reaching the maxi-

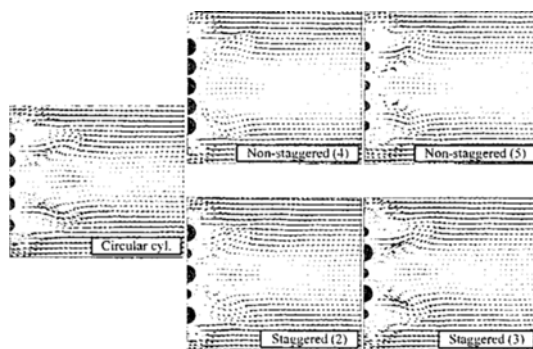


Fig. 7. Mean velocity distribution behind circular and wavy cylinders at $Re=1100$

imum; larger gaps are provided for the oncoming flow. Though, the deviation value in this plane is still larger than that in the staggered planes, especially in the areas corresponding to the jet flows around cylinder 3, indicating the swinging movements and the erratic flow speed of the jet flows in the saddle plane for non-staggered wavy cylinders arrangement.

One could deduce that the unsteady forces, which were produced by turbulent buffeting, exerted on the non-staggered wavy cylinders arrangement would be very fluctuating and unstable. Assuming the row of cylinders being considered as a heat exchanger tube row, the severe reverse flow of the nodal plane, that nearly blocks the oncoming flow to flow into the gaps, will also be a very undesirable feature of the flow. Therefore, the non-staggered wavy cylinders arrangement is not considered to be a suitable arrangement for closely packed tube bundles.

Lam et al. [13] reported that an elongation of the formation length will give rise to a higher back pressure in the rear side of a single cylinder, which is the most important contribution in producing a low drag force. It would be interesting to see whether the wavy cylinders will bring about the same effects to one row of side-by-side cylinders.

The formation length of each cylinder no longer exists due to wake interference. Instead, a statistically averaged vortex-pair in the wide wake behind cylinder 3 is formed as shown in Fig. 8. In Fig. 8, two foci (F_1 and F_2) of the vortex-pair and one saddle point (S_p), which denotes $\bar{u}/U_x=0$, are evidently formed for the circular cylinder and staggered wavy cylinder arrangement. Thus, the measurement of the vortex closure length could be applied based on the statistical average results. In this investigation, the wake vortex closure length (L_{vc}) is defined as the stream-wise distance between the centre of the middle cylinder and the saddle point S_p of wide wakes normalized by the mean diameter of the cylinder. In the cases shown in Fig. 8, it is apparent that the vortex closure length (L_{vc}) decreases with the increase of the Reynolds number for the circular and staggered wavy cylinders at such Re range.

The values of the L_{vc} of wavy and circular cylinders are listed in Table 1 for comparison. The bracketed numbers (2) and (3) are consistent with that in the Fig. 3. For low Reynolds number $Re < 800$, there is virtually not much difference in L_{vc} . However, for $Re \geq 1100$, a maximum of over 20% decrease in L_{vc} is found in the two planes of the staggered arrangement

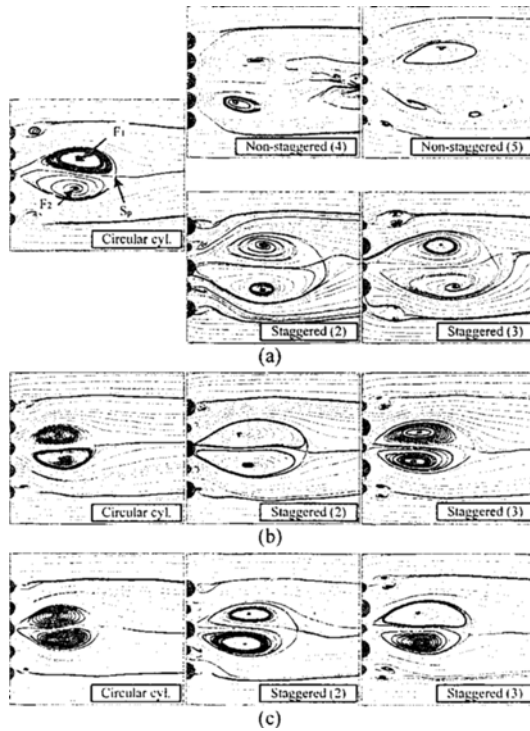


Fig. 8. Statistical mean streamline topologies of circular, staggered and non-staggered wavy cylinders, (a) $Re=1100$, (b) $Re=3800$, (c) $Re=20000$.

Table 1. Summary of wake vortex closure length L_{vc} for different Reynolds number at the measurement planes.

Re	L_{vc} of circular cyl.	L_{vc} of wavy cyl. (2)	L_{vc} of wavy cyl. (3)
125	23.2	22.3	22.5
500	22.4	22.2	21.5
800	21.6	21.4	21.3
1100	19.1	24.4	23.4
3800	16.3	21.5	20.0
20000	15.3	20.0	18.7
29000	13.2	16.6	15.2
40000	10.1	12.3	11.9

ment compared to that of the circular cylinder arrangement ($Re=3800$).

In general, a decrease of L_{vc} with Re is evidently observed for both circular cylinder and wavy cylinder arrangement. In the case of $Re \geq 1100$, the vortex closure length (L_{vc}) for the staggered wavy cylinder arrangement is longer than that of the circular cylinder.

Furthermore, it can be seen from Fig. 9 that the

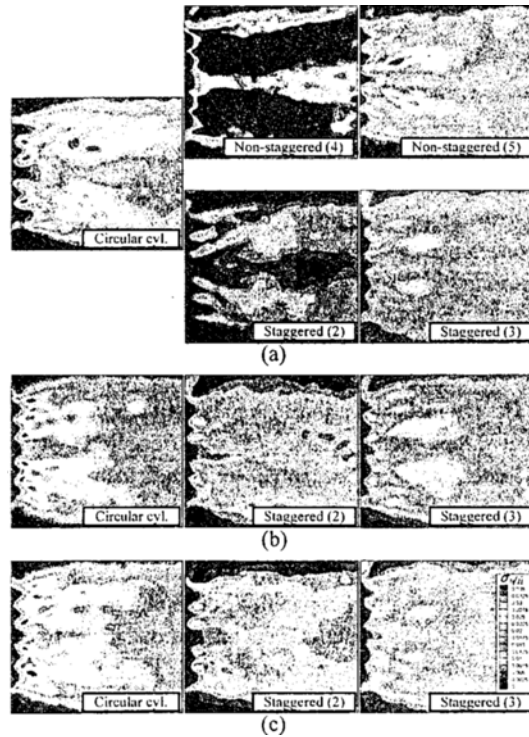


Fig. 9. Normalized standard deviation contours of velocity distribution behind the circular, staggered and non-staggered wavy cylinders, (a) $Re=1100$, (b) $Re=3800$, (c) $Re=20000$.

maximum deviation values of velocity distribution of the staggered wavy cylinders are at least 10% smaller than that of circular cylinders. The hot zones near the wavy cylinders could also be found to be smaller in comparison, which indicates the flow field behind the wavy cylinders is nearly stationary. In the case of circular cylinders, the deviation values reach a maximum adjacent to the circular cylinders. The hot zones extend to the wake downstream in strips. This may suggest that the flow-structure interactions among cylinders and flow are relatively more intensive.

Therefore, we may conclude that the staggered side-by-side wavy cylinder arrangement will most likely be able to suppress the unsteady nature of the flow field downstream of the cylinder row at sub-critical range of Reynolds number.

4. Conclusions

Experiments on the investigation of the characteristics of the near wakes of five side-by-side circular cylinder arrangement and wavy cylinder

arrangement with spacing ratio $T/d=1.5$, have been carried out in a water tunnel. The Reynolds number of the experiments covers a wide range from 125 to 40000.

Flow patterns of the wakes downstream of five side-by-side circular cylinders are studied. Flow visualization study indicates that due to flow interference at close cylinder spacing, individual Karman vortex shedding no longer exists behind every cylinder. As a result of wake interference, a typical flow pattern with a wide wake behind the middle cylinder is observed.

On the metastable issue, the results of experiments show the saddle plane of non-staggered wavy cylinders is very sensitive to disturbance of the oncoming flow; the circular cylinders take the second place especially when the Reynolds number is small. However, the staggered wavy cylinder arrangement could provide good capability in keeping away from metastable flow patterns. This may be due to the three dimensional flow introduced by the periodical variation of the cross-section of this arrangement. On the contrary, though the three-dimensional flow could also be identified in the non-staggered arrangement, the regular cross section variation and the alternating big and small gaps of the arrangement may excessively increase the local gradient of the flow speed value in the spanwise direction. The reverse flow that blocks the oncoming flow from entering the small gaps enhances the disturbance of the flow field. From discussions above, we conclude that the non-staggered side-by-side cylinders arrangement could only reinforce the unsteadiness pattern of the flow rather than minimize it. So, the non-staggered cylinders arrangement is not a suitable choice for the replacement of circular tubes in heat exchangers.

The PIV technique provides full field velocity distribution of measurement planes behind the cylinders. By compiling the statistical mean streamline map, a big vortex-pair is identified for the case of circular cylinder and staggered cylinder arrangement. The wake vortex closure length (L_{vc}) of circular cylinders and staggered wavy cylinders is measured. Combining the discussions of the velocity maps and the normalized standard deviation contours, we conclude that, in the range of Reynolds number studied, the staggered wavy cylinders are capable of producing a stable stationary flow pattern behind the cylinder row. This suggests the unsteadiness downstream of the cylinders could be suppressed by

introducing such arrangement of wavy cylinders. Furthermore, one could anticipate this arrangement would have an advantage in the suppression of flow induced vibration caused by the interaction among cylinders and fluid flow.

Acknowledgements

The authors wish to thank the Research Grants Council of the Hong Kong Special Administrative Region, China, for its support through Grant No. PolyU 5188/05E.

Nomenclature

- a : Amplitude of the surface curve of wavy cylinder
- d : Diameter/mean diameter of cylinders, m
- $F_{1,2}$: Foci points of vortex-pair
- H : Height of the test section of water tunnel, mm
- L : Length of the test section of water tunnel, mm
- L_{vc} : The wake vortex closure length
- Re : Reynolds number
- S_p : Saddle point of vortex-pair
- T : Transverse spacing, m
- U_∞ : Free stream velocity of the oncoming flow
- u : Streamwise velocity
- \bar{u} : Mean streamwise velocity
- v : Crosswise velocity
- W : Width of the test section of water tunnel, mm
- λ : Wave length of surface curve of wavy cylinder

References

- [1] M. M. Zdravkovich and K. L. Stonebanks, Intrinsically nonuniform and metastable flow in and behind tube arrays, *Journal of Fluids and Structures*. 4 (1990) 305-319.
- [2] A. Ahmed and B. Bays-Muchmore, Transverse flow over a wavy cylinder, *Physics of Fluids A4* (1992) 1959-1967.
- [3] A. Ahmed, M. J. Kahn and B. Bays-Muchmore, Experimental investigation of a three-dimensional bluff-body wake, *AIAA Journal*. 31 (1993) 559-563.
- [4] K. Lam et al., Three-dimensional nature of vortices in the near wake of a wavy cylinder, *Journal of Fluids and Structures*. 19 (2004) 815-833.
- [5] K. Lam and Y. F. Lin, Drag force control of flow over wavy (varicose) cylinders at a low Reynolds number, *Journal of Mechanical Science and Technology*. 21 (2007) 1331-1337.
- [6] S.-J. Lee and A.-T. Nguyen, Experimental investigation on wake behind a wavy cylinder

- having sinusoidal cross-sectional area variation, *Fluid Dynamics Research* 39 (2007) 292-304.
- [7] S. Corrsin, Investigation of the Behavior of Parallel two Dimensional Air jets, *NACA rep.* 4424 (1944).
- [8] B. W. Roberts, Low frequency, aero elastic vibrations in a cascade of circular cylinders, *IMEchE Mechanical Engineering Science Monograph.* 4 (1966).
- [9] C. F. Cowdrey, Some observations on the flow of air through a single row of parallel, *Closely Spaced Cylinders, Natl. Phys. Lab. Aeronaut.* 1064 (1968).
- [10] P. Bradshaw, The effect of wind tunnel screens on nominally two dimensional boundary layers, *Journal of Fluid Mechanics.* 22 (1965) 679-687.
- [11] M. Cheng and P. M. Moretti, Experimental study of the flow field downstream of a single tube row, *Experimental Thermal and Fluid Science.* 1 (1988) 69-74.
- [12] H. Akilli, A. Akar and C. Karakus, Flow characteristics of circular cylinders arranged side-by-side in shallow water, *Flow Measurement and Instrumentation.* 15 (2004) 187-197.
- [13] K. Lam et al., Experimental investigation of the mean and fluctuating forces of wavy (varicose) cylinders in a cross-flow, *Journal of Fluids and Structures.* 19 (2004) 321-334.